

# Rheological Predictions of Network Systems Swollen with Entangled Solvent

**Maria Katzarova**

Dept. of Chemical and Biological Engineering, and Center for Molecular Study of Condensed Soft Matter, Illinois Institute of Technology, Chicago, IL 60616

**Marat Andreev**

Dept. of Physics, Illinois Institute of Technology, Chicago, IL 60616

**Yelena R. Sliozberg**

U.S. Army Research Laboratory, Aberdeen Proving Ground, Aberdeen, MD 21005

Bowhead Science and Technology, King George, VA 22485

**Randy A. Mrozek, Joseph L. Lenhart, and Jan W. Andzelm**

U.S. Army Research Laboratory, Aberdeen Proving Ground, Aberdeen, MD 21005

**Jay D. Schieber**

Dept. of Chemical and Biological Engineering, Dept. of Physics, and Center for Molecular Study of Condensed Soft Matter, Illinois Institute of Technology, Chicago, IL 60616

DOI 10.1002/aic.14370

Published online February 2, 2014 in Wiley Online Library (wileyonlinelibrary.com)

*The mechanical properties of a cross-linked polydimethylsiloxane (PDMS) network swollen with nonreactive entangled PDMS solvent was previously studied experimentally. In this article, we use the discrete slip-link model to predict its linear and nonlinear rheology. Model parameters are obtained from the dynamic modulus data of pure solvent. Network rheology predictions also require an estimate of the fraction and architecture of dangling or inactive strands in the network, which is not directly measurable. The active strand fraction is estimated from dynamic modulus measurements, and the molecular weight is adjusted to fit the dynamic modulus data. Then, the nonlinear rheology can be predicted without adjustments. These successful predictions strongly suggest that the observed rheological modification in the swollen blend arises from the constraint dynamics between the network chains and the dangling ends. © 2014 American Institute of Chemical Engineers AICHE J, 60: 1372–1380, 2014*

We dedicate this article to Prof. R. Byron Bird on the occasion of his 90th birthday. We attempt to follow the twin exhortations of Bob to be both mathematically rigorous and practically relevant.

**Keywords:** *rheology, polymer properties, gels, networks, mathematical modeling, multiscale modeling*

## Introduction

Cross-linked polymer networks swollen with polymeric solvent have shown adaptive mechanical response. This frequency dependent response makes these gels desirable for applications such as tissue simulants for ballistic testing.<sup>1</sup> Recently, the dependence of solvent molecular weight and concentration on the mechanical and rheological properties of an end-linked polydimethylsiloxane (PDMS) gel that contains PDMS soluble material were studied by Mrozek et al.<sup>2</sup> In that work, the focus was on an end-functionalized PDMS precursor that is much larger than the entanglement molecu-

lar weight, resulting in a low chemical-cross-link density and a modulus that is determined by the degree of entanglement. As a result, a change in the entanglement screening or enhanced looped formation will have a significant impact on the mechanical properties of the gel. The networks are formed in the presence of nonreactive PDMS solvents with molecular weights broadly spanning the molecular weight of entanglement for PDMS. The increased frequency dependence of the mechanical response and improved gel fracture toughness with entangled solvent is expected to benefit many applications including electronic device encapsulation, pressure sensitive adhesives, and tissue surrogates for biomedical engineering.

Gels swollen with high-molecular-weight solvent were previously modeled using standard polymer coarse-grained, bead-spring “Kremer–Grest” models.<sup>3–5</sup> These simulations

Correspondence concerning this article should be addressed to J. D. Schieber at [schieber@iit.edu](mailto:schieber@iit.edu).

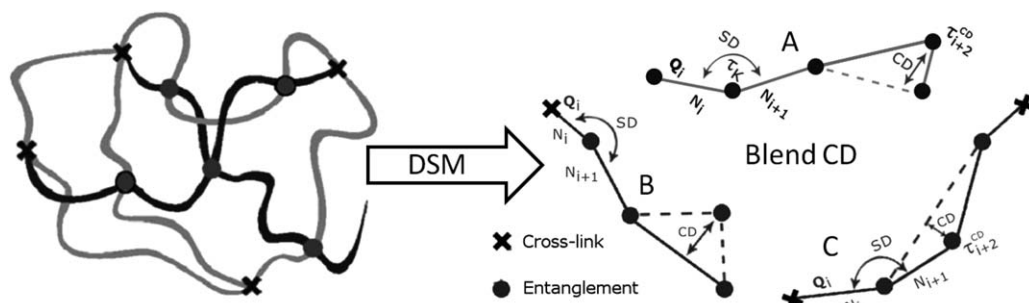


**Figure 1. Sketch of how the swollen PDMS network is modeled using the DSM.**

In the DSM, each component is simulated independently using a self-consistent mean field that accounts for the effect of other types of chains. The components of the swollen network modeled here are, A: SC, B: DC, C: NC. The circles represent binary entanglements and the crosses represent cross-links. Both of which are fixed in space for Green-Kubo calculations or moved affinely for flow.

have proven to be a useful technique to study microscopic topology and dynamics of lightly to moderately entangled polymer systems. However, the models have limitations when studying very high-molecular-weight polymer chains where entanglement dynamics become dominant, because the time scales of interest are frequently longer than what is reachable computationally. Attempts have also been made to apply tube models<sup>6,7</sup> to describe the elasticity of both dry<sup>8,9</sup> and swollen<sup>10,11</sup> polymer networks. However, the time-dependent entanglement effect on the relaxation of polymeric networks remains unresolved in those theories.<sup>12</sup>

In this article, we apply the discrete slip-link model (DSM) introduced by Schieber and coworkers,<sup>13–17</sup> which was developed to describe the dynamics of flexible entangled polymer liquids and gels. The model is able to predict the linear viscoelasticity of monodisperse linear, polydisperse linear, and branched systems. Recently, the model also showed mostly good agreement with dielectric relaxation experiments.<sup>18</sup> Without any adjustment, the DSM shows excellent agreement with shear flow experiments and elongational flows with elongation ratios of up to 10–20, as shown recently.<sup>19</sup>

The model was first applied to cross-linked polymer gels with entanglement dominated dynamics by Jensen and coworkers.<sup>20</sup> In that work, the effect of network imperfections (dangling network chains) on the dynamic modulus of the gels was systematically studied using the DSM.

In this article, we expand on that work and use the DSM to estimate the composition and predict the relaxation and nonlinear mechanical response of cross-linked polymer networks swollen with polymeric solvent. The main objective is to test a methodology for predicting and designing the rheological properties of gels. Toward this end, we test the feasibility of using the model to characterize the fraction of gel strands that are active from the dynamic modulus, and check if the nonlinear rheology can then be predicted. The experimental system modeled is a cross-linked PDMS network in the presence of high-molecular weight PDMS linear solvent. When accounting for imperfections in the cross-linked network, this application requires the coupling of three categories of architectures: (1) entangled network chains (NC); (2) dangling network chains (DC); and (3) entangled solvent chains (SC). Additionally, we account roughly for the polydispersity in the molecular weight distribution of each of the components in the network blend.

The article is organized as follows, in Model: DSM for Blends Section, we summarize the main aspects of the DSM

with an emphasis on how the interaction between different types of chain architectures and molecular weights are handled in the single-chain self-consistent mean-field approach. In Blend Composition Section, the details about the composition of the system being modeled are presented. There, we describe the way in which we account for the polydispersity of each component in the network blend. Also, the methodology to estimate the fraction of imperfections in the network structure (dangling chains) is described. In Determination of the DSM Parameters for PDMS Section, the two parameters that are required in the DSM to predict rheological properties are estimated using dynamic modulus data for polydisperse entangled PDMS liquid. These same parameters can then be used to model all other PDMS chain architectures and molecular weights. In Dynamic Modulus Predictions of the Swollen Network Section, the dynamic modulus of a cross-linked PDMS network swollen with polymeric PDMS solvent is predicted using the DSM and compared to experimental data by adjusting the only remaining parameter: the molecular weight of the dangling network chains. An analysis on the effect of high-molecular-weight solvent in the linear viscoelastic response of cross-linked polymer networks is given. In Predictions of Simple Elongation of Swollen Network Section, a simple elongation experiment of the swollen PDMS network is tested against the DSM prediction. Moreover, important insight into the specific dynamics of each component in this complex blend is gained.

## Model: DSM for Blends

The DSM is a single-chain mean-field model for entanglement-dominated polymer dynamics proposed by Schieber et al.<sup>14</sup> and evolved by Khaliullin and Schieber.<sup>16</sup> After a brief outline, we apply the model to polymeric gels swollen with high-molecular-weight solvent.

The network and solvent chains are described by random walk statistics. This is expected to hold for polymeric chains with contour length and entanglement spacing larger than several Kuhn steps. The model is a single-chain mean-field model, where Figure 1 shows cartoons of the coarse-graining process of the real network and solvent chains. The chains are first coarse-grained by random walk statistics; then, they are further coarse-grained to the primitive path defined by the entanglements, assuming that the chain relaxation is slower than the relaxation of a strand between entanglements. The entanglements are randomly distributed

along the chain with uniform probability  $1/(1+\beta)$ , where  $\beta$  is a model parameter related to the entanglement density. The primitive path defines the entanglement spacing. The number of Kuhn steps,  $N_i$ , in the  $i$ th strand fluctuates due to Kuhn step shuffling through the slip-links, a process called “sliding dynamics” (SD). When this process occurs at the ends of a solvent chain, or at the uncross-linked end of a dangling chain, entanglements can be destroyed or created.

At equilibrium, the probability density for a given chain conformation is governed by the modified Maxwell–Boltzmann relation,<sup>16</sup>  $p_{\text{eq}}^\gamma(\Omega)$  where  $\gamma$  denotes chain length and  $\Omega \equiv (Z, \{N_i\}, \{\mathbf{Q}_i\}, \{\tau_i^{\text{CD}}\})$  determines the chain conformation in the level of description of the DSM. Where  $Z$  is the number of entangled segments, and  $\mathbf{Q}_i$  is the vector connecting entanglements  $i-1$  and  $i$ .  $p_{\text{eq}}^\gamma(\Omega)$  is given by

$$p_{\text{eq}}^\gamma(\Omega) = \frac{\delta(N_K^\gamma, \sum_{i=1}^Z N_i)}{J\beta^{Z-1}} \exp \left[ -\frac{F(\Omega)}{k_B T} \right] \prod_{i=1}^{Z-1} p^{\text{CD}}(\tau_i^{\text{CD}}) \quad (1)$$

where  $J = (1 + 1/\beta)^{N_K^\gamma - 1}$  is the normalization constant,  $\delta(i, j) = \delta_{ij}$  is the Kronecker delta function which is responsible for the conservation of Kuhn steps in a chain,  $N_K^\gamma$  is the total number of Kuhn steps in a chain of type,  $\gamma$ ,  $F(\Omega)$  is the free energy of a chain with conformation  $\Omega$ ,  $p^{\text{CD}}(\tau^{\text{CD}})$  is the constraint dynamics (CD) probability density of entanglement lifetimes, which in the mean-field description accounts for the creation and destruction of entanglements anywhere along the chain,  $k_B$  is Boltzmann’s constant, and  $T$  is the absolute temperature.

The random walk of  $N_i$  Kuhn steps between two slip-links of separation  $|\mathbf{Q}_i| = Q_i$  can be approximated by a Gaussian free energy derived by Schieber et al.<sup>14</sup>

$$\frac{F_s(\mathbf{Q}_i, N_i)}{k_B T} = \frac{3Q_i^2}{2N_i a_K^2} + \frac{3}{2} \ln \left[ \frac{2\pi N_i a_K^2}{3} \right] \quad (2)$$

where  $a_K$  is the length of a Kuhn step. The free energy for a chain is the sum of the free energies of the segments in the chain

$$F(\Omega) = \sum_{i=1}^{Z-\alpha} F_s(\mathbf{Q}_i, N_i), \quad (3)$$

where  $\alpha$  takes a value of 0 for a network chain, 1 for a dangling chain, and 2 for a solvent chain. For a network chain, both strand ends are fixed and accounted for in the free energy of the chain. For the dangling chain, only one end strand is fixed. And for the solvent chain, neither end strand contributes to the chain free energy. This is because the end strand samples all possible orientations, averaging to a zero free energy. The free energy of an entangled strand, Eq. 2, is valid for polymer chains which are not stretched beyond approximately 1/3 of their contour length.

The entanglement activity of the surrounding chains is responsible for fluctuations in the number of entanglements on the chain. At equilibrium, Kuhn-step shuffling between entangled strands is due to Brownian forces and free energy differences.

The characteristic lifetime of the  $i$ th entanglement,  $\tau_i^{\text{CD}}$ , is introduced to implement a mean-field self-consistent realization with independent chains in the ensemble. The lifetimes  $\tau_i^{\text{CD}}$  are chosen from the distribution of lifetimes,  $p^{\text{CD}}$ . This

distribution is determined self-consistently from destruction of entanglements in a system by SD. Entanglements between two entangled network chains are permanently trapped; hence,  $\tau_i^{\text{CD}}$  is infinitely large and for those  $p_{\text{NC}}^{\text{CD}}(\tau^{\text{CD}}) = 2\delta(1/\tau^{\text{CD}})/(\tau^{\text{CD}})^2$ . The  $p^{\text{CD}}$  for the swollen network blend considered in this work is given by

$$p^{\text{CD}}(\tau^{\text{CD}}) = w_{\text{DC}} \sum_{\gamma=1}^{N_{\text{DC}}} w_\gamma^{\text{DC}} p_{\text{DC},\gamma}^{\text{CD}} + w_{\text{SC}} \sum_{\gamma=1}^{N_{\text{SC}}} w_\gamma^{\text{SC}} p_{\text{SC},\gamma}^{\text{CD}} + w_{\text{NC}} \sum_{\gamma=1}^{N_{\text{NC}}} w_\gamma^{\text{NC}} p_{\text{NC},\gamma}^{\text{CD}} \quad (4)$$

where  $N$  is the number of components in the polydisperse distribution of molecular weights of each type of architecture in the blend. Destruction and creation of entanglements by CD occur anywhere along the chain, which is different from creation and destruction of entanglements by SD which can only occur in dangling ends. Therefore, in network chains in a blend, such as the one considered here, entanglements can be created and destroyed by CD. In the dangling chains of the network (network imperfections), entanglements can be created and destroyed by SD only in the uncross-linked end and by CD anywhere along the chain. For the solvent chains, entanglements are created and destroyed by SD on both ends of the chain and by CD anywhere along the chain.

Therefore, in the DSM each component of the swollen network blend is modeled in a self-consistent realization with independent chains in the ensemble. The effect of other chains is given by the self-consistent mean-field defined in Eq. 4. This concept is illustrated in Figure 1. In other words, in the DSM, each component of the complex swollen network blend, with different architectures and polydispersity in each of the components, can be realized independently while the effect of other architectures and molecular weights is given by the CD mean-field.

The probability density in Eq. 1 evolves in time according to a differential Chapman–Kolmogorov equation.<sup>13</sup> Two types of calculations can be performed, equilibrium (or Green–Kubo) calculations in which the rate of deformation tensor<sup>21,22</sup> is set to zero and the autocorrelation function of stress at equilibrium is followed; or flow calculations in which a specific flow field is applied and the stress as a function of time is recorded.

The stress tensor is obtained from thermodynamics<sup>23</sup>

$$\boldsymbol{\tau} = \sum_{\gamma=1}^N \boldsymbol{\tau}_\gamma, \quad \boldsymbol{\tau}_\gamma(t) = -n_\gamma \left\langle \sum_{i=1}^{Z-\alpha} \mathbf{Q}_i \left( \frac{\partial F(\Omega)}{\partial \mathbf{Q}_i} \right)_{T, \{N_i\}, \{\mathbf{Q}_{j \neq i}\}} \right\rangle_\gamma \quad (5)$$

where  $\alpha$  has value 0 for a network chain, 1 for a dangling chain, and 2 for a solvent chain. After calculating  $p^{\text{CD}}(\tau^{\text{CD}})$  and using it in Eq. 1, the relaxation modulus of the blend,  $G(t)$  is predicted using the Green–Kubo expression

$$G_\gamma(t) = \frac{1}{n_\gamma k_B T} \langle \tau_{xy}(0) \tau_{xy}(t) \rangle_{\text{eq}, \gamma} \quad (6)$$

where  $\langle \dots \rangle_{\text{eq}}$  is an ensemble average,  $\tau_{xy}(t)$  can be any off-diagonal stress tensor component, and  $n_\gamma$  is the number of chains per unit volume. Note that the stress tensor of the system is a sum of the stresses of its individual chains per unit volume as can be seen in Eq. 5. From this, it follows that the relaxation modulus of the blend can be expressed in

**Table 1. Molecular Characteristics and Parameters for the GEX of the Nonreactive PDMS Soluble Solvent Chains (m-PDMS) and Gel Precursor Chains (v-PDMS)**

Name	$M_w$ (kDa)	$M_N$ (kDa)	$M_w/M_N$	$M_z$ (kDa)	$m_p$	$a$	$b$
m-PDMS	187.5	116.8	1.61	263.7	35074.1	2.057	0.810
v-PDMS	116.1	74.8	1.55	165.7	1984.09	3.535	0.536

terms of the relaxation modulus of each of the components in the blend as

$$G(t) = w_{DC} \sum_{\gamma=1}^{N_{DC}} w_{\gamma}^{DC} G_{\gamma}^{DC}(t) + w_{SC} \sum_{\gamma=1}^{N_{SC}} w_{\gamma}^{SC} G_{\gamma}^{SC}(t) + w_{NC} \sum_{\gamma=1}^{N_{NC}} w_{\gamma}^{NC} G_{\gamma}^{NC}(t) \quad (7)$$

## Blend Composition

One of the main challenges is to model a blend with complex and partially unknown composition. More specifically, here, we consider a realistic network with imperfections. These imperfections are caused by incomplete cross-linking during curing or structures that are not active. Additionally, most commercially available precursors and high-molecular-weight solvents have significant polydispersity in their molecular weight distributions. In this section, we propose a procedure to quantify approximately these two compositional parameters theoretically.

The specific system to be modeled was studied experimentally by Mrozek et al.<sup>2</sup> and is composed of a gel formed by a vinyl-terminated v-PDMS precursor that is much larger than the entanglement molecular weight resulting in a low chemical cross-link density and a modulus that is determined by the degree of entanglement. The networks are formed in the presence of nonreactive PDMS methyl-terminated m-PDMS solvents broadly spanning the molecular weight of entanglement for PDMS. The samples are cured for 72 h at 82°C in the presence of a platinum-cyclcovinylmethylsiloxane complex.

Our goal is to predict simultaneously the dynamic modulus and elongation experiments of one of the swollen network blends studied experimentally by Mrozek et al.<sup>2</sup> In that article, PDMS networks with different amounts of high-molecular-weight PDMS solvent were prepared. Here, we focus on the blend with 50% loading of high-molecular-weight solvent.

## Polydispersity of components

The molecular weight distribution (MWD) of the precursor chains and the PDMS solvent chains can be measured experimentally using gel permeation chromatography. For the specific system studied in this article, the results of these measurements are shown in Table 1. The molecular weight distribution obtained from these experiments can be fit to a generalized exponential function (GEX)<sup>24</sup>

$$W(M) = \frac{b}{\Gamma\left(\frac{a+1}{b}\right)} \left(\frac{M}{m_p}\right)^{a+1} \exp\left[-\left(\frac{M}{m_p}\right)\right] \quad (8)$$

where the parameters,  $m_p$ ,  $a$ , and  $b$ , listed in Table 1, are related to the moments:  $M_N = m_p \frac{\Gamma\left(\frac{a+1}{b}\right)}{\Gamma\left(\frac{a}{b}\right)}$ ,  $M_w = m_p \frac{\Gamma\left(\frac{a+2}{b}\right)}{\Gamma\left(\frac{a+1}{b}\right)}$ ,  $M_z = m_p \frac{\Gamma\left(\frac{a+3}{b}\right)}{\Gamma\left(\frac{a+2}{b}\right)}$ .

Note that the solvent is long enough to entangle, as  $M_e \cong 29$  kDa for PDMS chains.<sup>2</sup> The MWD for the v-PDMS precursors are shown in Figure 2B and the MWD for the m-PDMS chains are shown in Figure 2A.

It is convenient to approximate the GEX distribution with a set of discrete molecular weights for calculating rheology. The simplest discrete approximation is bidisperse, where the first and second moments were matched. We find this simple approximation to be sufficient to reproduce experimental results. In principle, one can use a discrete approximation of the GEX function with as many molecular weights as necessary to obtain a good prediction of experimental results. However, this also increases the computational cost. The bidisperse approximations are plotted together with the GEX fit of the molecular weight distribution for the solvent and precursor chains in Figures 2A, B, respectively.

The molecular weight distribution of the dangling network chains must also be estimated, which cannot be measured experimentally, therefore, we model them as monodisperse chains with a molecular weight chosen to obtain good

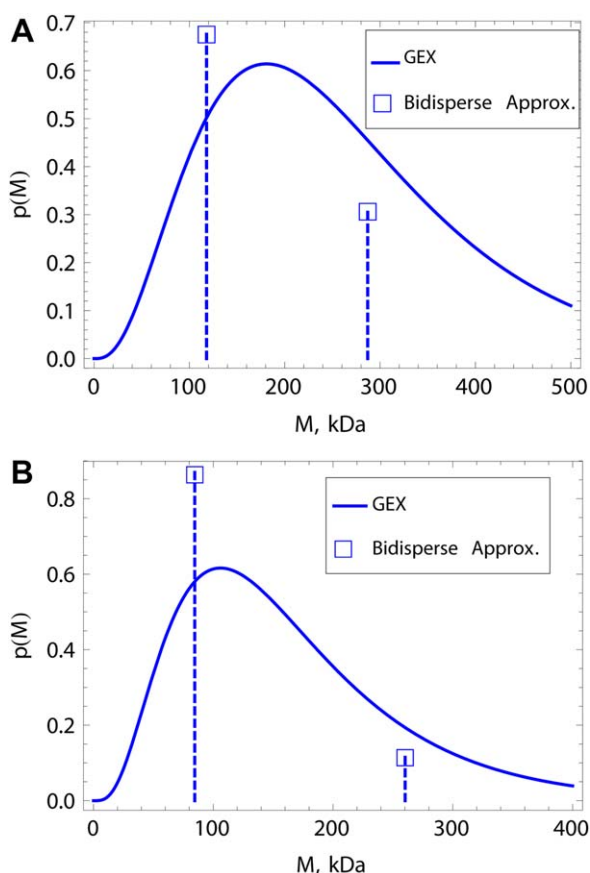


**Figure 2. (A) Bidisperse approximation of the molecular weight distribution of solvent chains,  $M_w^{SC1} = 118.1$  kDa,  $w_1^{SC} = 0.7$  and  $M_w^{SC2} = 287$  kDa,  $w_2^{SC} = 0.3$ .**

The solid curves represent the continuous GEX for the nonreactive PDMS soluble chains (m-PDMS) whose parameters are listed in Table 1. (B) Bidisperse approximation of the molecular weight distribution of network chains,  $M_w^{NC1} = 84.6$  kDa,  $w_1^{NC} = 0.87$  and  $M_w^{NC2} = 260.2$  kDa,  $w_2^{NC} = 0.13$ . The solid curves represent the continuous GEX for the reactive network precursor chains (v-PDMS) whose parameters are listed in Table 1. [Color figure can be viewed in the online issue, which is available at [www.interscience.wiley.com](http://www.interscience.wiley.com).]



agreement with the relaxation processes observed in the experimental dynamic modulus data for the swollen networks. We find that dangling chains with a molecular weight of 187.5 kDa represent the experimental  $G^*$  data reasonably well.

### Fraction of dangling chains

Additionally, the volume fraction of precursor chains that are not fully cross-linked during the curing process is also unknown. To estimate this fraction, we use results of Jensen and coworkers.<sup>20</sup> In that work, it was shown that the low-frequency plateau is a linear function of the density of cross-links plus trapped entanglements. Hence, its value is a strong function of the mass fraction of active structures in the network, in agreement with classical theories. Using the DSM, several systems with different cross-link densities were simulated, and an empirical relation between the elastic plateau and the fraction of the dangling structures was developed. In this work, we generalize this equation to a bidisperse network as

$$G_{0,ana} = \frac{w_{NC}}{1-w_{SC}} \left[ \frac{\rho RT}{M_{w1}^{NC1}} (0.74Z_{T,1} + 1) w_1^{NC} + \frac{\rho RT}{M_{w2}^{NC2}} (0.74Z_{T,2} + 1) w_2^{NC} \right] \quad (9)$$

where  $Z_{T,\gamma}$  is the average number of trapped entanglements, defined as

$$Z_{T,\gamma} = \frac{w_{NC}}{1-w_{SC}} \left( \frac{N_K^{NC,\gamma} + \beta}{\beta + 1} - 1 \right) \quad (10)$$

In Eqs. 9 and 10,  $w_{NC}$  is the fraction of network chains, and  $w_{SC}$  is the fraction of solvent chains which is known as it is specified for a given loading formulation. For the calculations performed in this article,  $w_{SC} = 0.5$  and  $w_1^{NC}$  and  $w_2^{NC}$  are the fractions of network strands of the bidisperse distribution of network strands shown in Figure 2B.

To estimate  $w_{NC}$ , we use the unloaded network elastic modulus ( $G_0 = G'(\omega \rightarrow 0) \approx 68 \text{ kPa}$ ) reported by Mrozek et al.<sup>2</sup> Using Eq. 9, our estimate for  $\beta$  (whose estimation we discuss in Determination of the DSM Parameters for PDMS Section), and the molecular weight distribution discussed in Blend Composition Section, we solve Eq. 9 for  $w_{NC}$ . For the specific system being considered, the fraction of network chains is found to be  $w_{NC} \cong 0.32$  and the fraction of dangling network chains is, therefore,  $w_{DC} \cong 0.18$ .

### Determination of the DSM Parameters for PDMS

The three input parameters for the DSM are the number of Kuhn steps,  $N_K$ ; the entanglement activity,  $\beta$ ; and the characteristic Kuhn step time,  $\tau_K$ .  $N_K$  can be calculated using  $N_K = M_w/M_K$ , where  $M_K$  is the molecular weight of a Kuhn step, reported to be 381 Da for PDMS.<sup>25</sup>

The DSM parameters for PDMS,  $\beta$  and  $\tau_K$ , are determined by fitting the simulation results to dynamic modulus experimental measurements for the pure solvent used to load the network. Dimensionless relaxation modulus results using the DSM are shown in Figure 3A for each of the two molecular weights in the bidisperse molecular weight distribution of the solvent chains. A modified Baumgaertel, Schausberger, and Winter (BSW) function<sup>26</sup> is used to fit the simulation results in the time domain. This function can then be analytically transformed to the frequency domain to obtain the

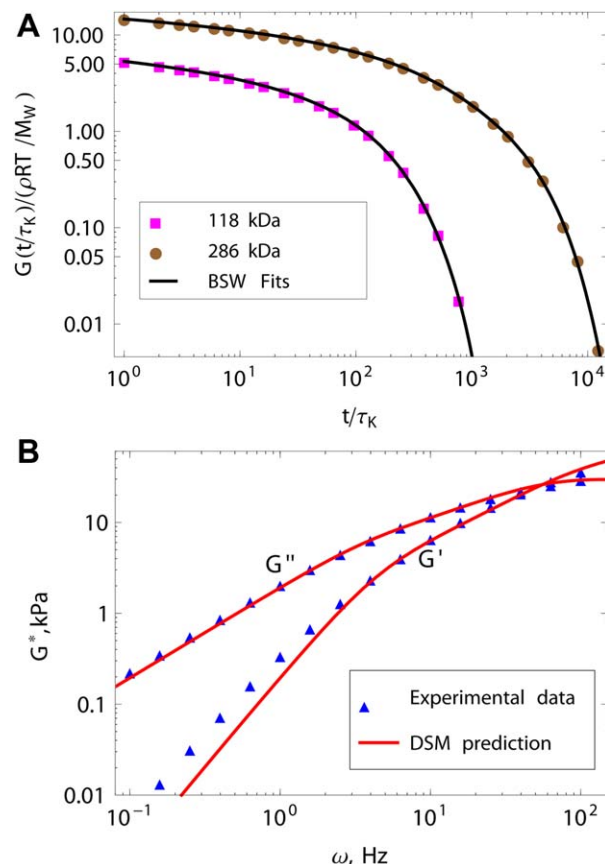


**Figure 3. (A) Relaxation moduli for the two components of the bidisperse approximation of the entangled solvent ( $N_{c,SC1}=16$  and  $N_{c,SC2}=43$ ).**

The symbols represent predictions by the DSM of the individual components of the bidisperse approximation of the molecular weight distribution of the m-PDMS chains. The solid lines represent a fit of the simulation results by a BSW spectrum. (B) Comparison of the DSM prediction for the pure entangled solvent with the experimental data (symbols). [Color figure can be viewed in the online issue, which is available at [wileyonlinelibrary.com](http://wileyonlinelibrary.com).]

dynamic modulus shown in Figure 3B.  $\beta$  was estimated to be 34.8. As the entanglement plateau is not observed in the frequency data, there is some uncertainty in this value but the prediction agrees well in the region of frequencies reported.  $\tau_K$  was simultaneously estimated during this fit to experimental data to be 0.026  $\mu\text{s}$ . Both of these values are architecture and molecular-weight independent.

Furthermore, in a parallel work by Andreev et al.,<sup>27</sup> it has been shown that a less detailed level of description than the DSM can be used to get quantitative predictions at greatly reduced cost. The Clustered Fixed Slip-Link Model is the DSM with fixed  $\beta=1$  and  $N_c$  instead of  $N_K$  and  $\tau_c$  instead of  $\tau_K$ .  $N_c$  as a function of  $N_K$  and  $\beta$  is given by

$$M_c \approx 0.56(\beta+1)M_K \quad (11)$$

and  $\tau_c$  as a function of  $\tau_K$  is given by

$$\tau_c \approx 0.265\beta^{8/3}\tau_K \quad (12)$$

Predictions with  $\beta=1$  were done with coarse-grained parameters  $N_{c,NC1}=12$  and  $N_{c,NC2}=34$ ,  $N_{c,SC1}=16$  and  $N_{c,SC2}=37$ , and  $N_{c,DC}=25$ . The results obtained are identical to the original, unscaled model.

## Dynamic Modulus Predictions of the Swollen Network

Using the model parameters found in Determination of the DSM Parameters for PDMS Section, we can now construct the self-consistent CD mean field according to Eq. 4. Then, each type of chain in the ensemble (irrespective of architecture and molecular weight) can be simulated independently using this blend  $p^{\text{CD}}$  field, Eq. 4.

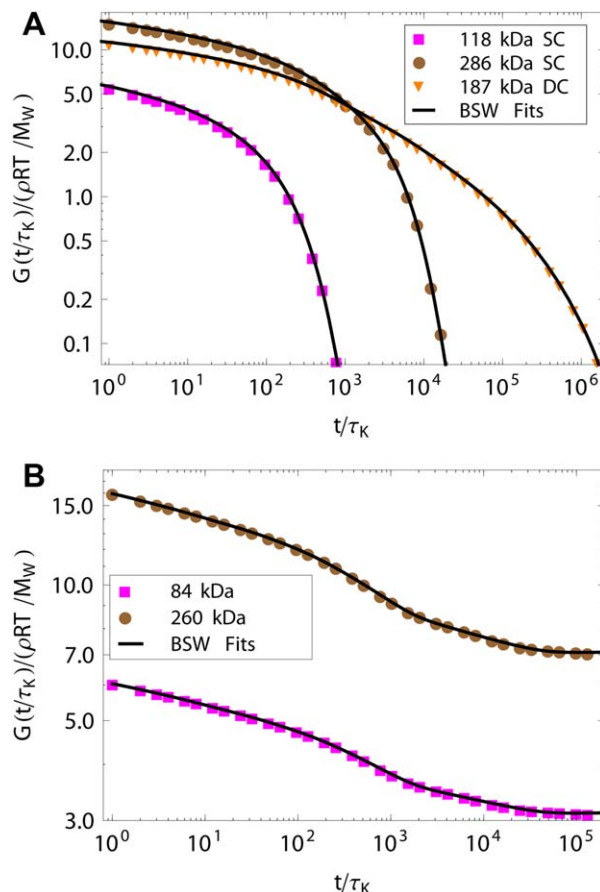
### Blend predictions

Figure 4A shows the dimensionless relaxation moduli obtained from these same simulations for the solvent chains in the presence of the blend CD field. It can be observed that the longer molecular weight in the bidisperse approximation has a long relaxation time as expected. Figure 4B shows the dimensionless relaxation moduli for the network chains in the same blend CD field. The relaxation dynamics are the same for both molecular weights as in the network chains, relaxation occurs only from CD, and these CD are the same for both molecular weight chains. A BSW function is used to fit the simulation results in the time domain. These functions are analytically transformed to the frequency domain to obtain the dynamic modulus.

Figure 4A also shows the dimensionless relaxation modulus for the dangling chains in the presence of the same blend CD field. Compared to the solvent, the dangling chains have a much longer relaxation time as they are fixed at one end to the network, and SD can only create and destroy entanglements at one end of the chain.

The relaxation modulus for each architecture, solvent chains, dangling network chains, and network chains, can then be constructed by performing a weighted average, Eq. 7, of the relaxation moduli of all the molecular weights, for each architecture, using the weight fractions found in Blend Composition Section. The dynamic modulus is then obtained by transforming the relaxation modulus to the frequency domain analytically. The resulting dynamic moduli for each of the different architectures in the swollen network blend are shown in Figure 5A. Note that the crossover for the dangling chains, which is a rough indicator of the longest relaxation time, occurs at much lower frequencies than that for the solvent chains. This is to be expected as the dangling chains are similar to star-branched melts, which can not relax by SD at the end fixed to the network. For the dangling and solvent chains, the entanglement plateau can be observed at high frequencies. It can also be observed that for the network component the storage modulus and the loss modulus do not crossover, as expected. For the network, an entanglement plateau is observed at high frequencies, and an elastic plateau is observed at low frequencies. Note that the contribution of the entangled solvent to the dynamic modulus of the blend is only relevant at high frequencies since at lower frequencies the solvent chains have relaxed significantly and the relative magnitude of their modulus with respect to network and network dangling chains becomes very small. Observe that at frequencies around  $10^1$  Hz the  $G''$  of the swollen network blend becomes dominated by the  $G''$  of the entangled solvent. The overall effect of the high molecular weight solvent is to increase energy dissipation at high frequencies while having a negligible effect on the mechanical properties at lower frequencies.

The dynamic modulus of the swollen network blend is calculated using Eq. 7, with  $w_{\text{SC}}=0.5$ ,  $w_{\text{DC}}=0.18$ , and



**Figure 4. (A) Relaxation moduli for the two components of the bidisperse approximation of the SC, and of the monodisperse approximation of the dangling chains (DC), with blend CD Eq. 4.**

**(B) Relaxation moduli for the two components of the bidisperse approximation of the network chains with self-consistent blend CD Eq. 4. [Color figure can be viewed in the online issue, which is available at [wileyonlinelibrary.com](http://www.interscience.wiley.com).]**

$w_{\text{NC}}=0.32$ , and the dynamic moduli for each of the individual architectures shown in Figure 5A. The result is shown in Figure 5B. Recall that the modulus for each architecture is simulated independently, but with a self-consistent  $p^{\text{CD}}$  field that accounts for the presence of all the components of the blend. The agreement with the experimental data is good and could potentially be improved by increasing the number of molecular weights in the discrete approximation of the GEX distributions of the molecular weights of each of the components of the blend, at increased computational cost. Noting the offset from the experimental data, suggests that our estimate for  $\beta$  may be a bit high. Nonetheless, we observe that the shape is captured well. For instance, in  $G'$ , the slight upturn at higher frequencies, which is caused by the increasing contribution of entangled solvent chains, is captured correctly by the model. In  $G''$ , the characteristic power-law behavior at intermediate and low frequencies is also predicted correctly by the model.

### Predictions of Simple Elongation of Swollen Network

We can now predict the nonlinear rheology without parameter adjustments. Simple elongation experiments for

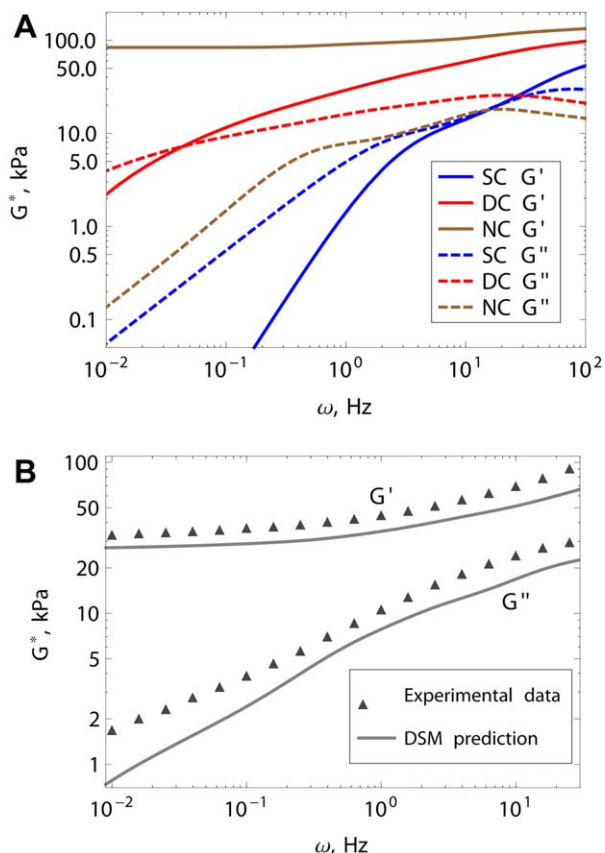


**Figure 5. Dynamic modulus of the swollen network blend.**

(A) Dynamic modulus of each component in the blend with self consistent blend CD. SC: Solvent chains; DC; NC. (B) Comparison of the DSM prediction for the swollen network blend with the experimental data of Mrozek et al.<sup>2</sup> [Color figure can be viewed in the online issue, which is available at [wileyonlinelibrary.com](http://wileyonlinelibrary.com).]

the same swollen PDMS network were reported by Sliozberg et al.<sup>3</sup> In these experiments, a dog-bone shaped sample of initial length  $L = 1$  in. is elongated at cross-head speeds between 0.05 and 5 in./s using a MTS 810 servo-hydraulic load frame. In this type of experiment, the elongation ratio of the sample,  $\lambda(\lambda = l/L)$ , is given by

$$\lambda = \dot{\lambda}t + 1 \quad (13)$$

where  $l$  is the length of the sample during the experiment and  $\dot{\lambda}$  is the elongation rate.

The elongation ratio is related to the Hencky strain,  $\epsilon$ , by<sup>22</sup>

$$\epsilon = \log(\lambda) \quad (14)$$

and consequently the Hencky strain rate can be expressed as

$$\dot{\epsilon} = \frac{\dot{\lambda}}{\lambda t + 1} = \frac{1}{t + 1/\lambda} \quad (15)$$

which is used in the DSM algorithm to construct the velocity gradient,<sup>22</sup> for simple elongation.<sup>21</sup>

Here, we attempt to predict the experimental results for three stretch rates, 5, 0.5, and 0.05 1/s. The simulation results for each of the architectures of the swollen network blend in simple elongation for the highest rate are shown in

Figure 6A. Just as was done for the Green–Kubo simulations presented in Dynamic Modulus Predictions of the Swollen Network Section, in this case too, each chain in the ensemble is simulated independently in a self-consistent CD mean field, Eq. 4, that accounts for the presence of chains with different architectures and molecular weights. It can be observed that the stress contribution from network chains is much larger than the contribution from dangling network chains and solvent chains.

The average swollen network response is obtained by calculating the weighted average of the individual stresses shown in Figure 6A, using the weight fractions found in Blend Composition Section,  $w_{SC}=0.5$ ,  $w_{DC}=0.18$ , and  $w_{NC}=0.32$ . The result is shown in Figure 6B, together with the experimental data reported by Sliozberg et al.<sup>3</sup> It can be observed that the model predicts the experimental data well with small deviations for  $\lambda \geq 5$ . To explain the fact that the high-molecular-weight solvent does not have a significant contribution to the overall mechanical response of the swollen gel, we estimated the Weissenberg number for this component during the experiment done at 5 1/s elongation rate. For the solvent component of the system, the longest

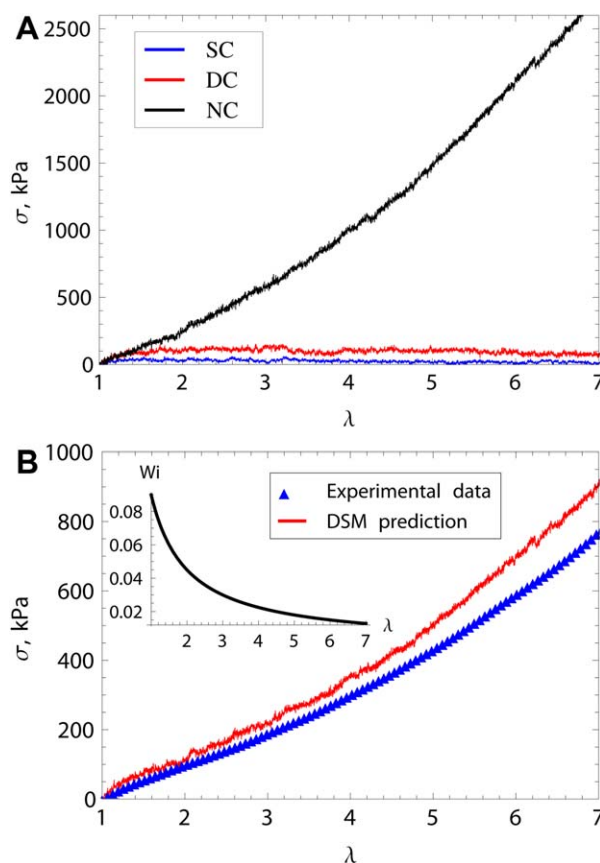


**Figure 6. (A) DSM prediction for simple elongation for each of the components of the PDMS swollen network blend in self-consistent blend CD.**

The figure shows the elongational stress,  $\sigma$ , as a function of the elongation ratio,  $\lambda$ . (B) Comparison with experimental data where the inset shows the Weissenberg number for uniaxial extension for the solvent component of the system modeled in Determination of the DSM Parameters for PDMS Section,  $\dot{\lambda}=5$  1/s,  $\tau_d=0.02$ s. [Color figure can be viewed in the online issue, which is available at [wileyonlinelibrary.com](http://wileyonlinelibrary.com).]



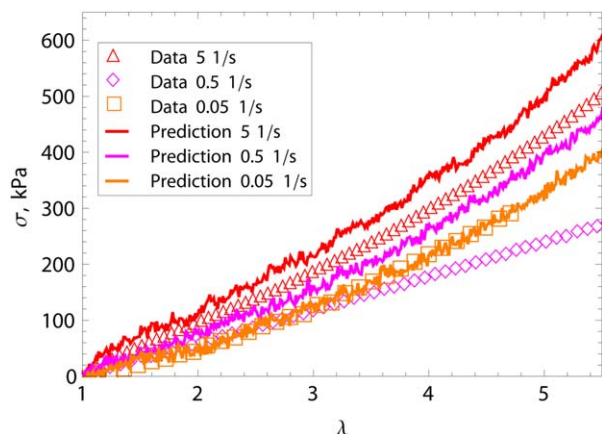


**Figure 7. Comparison of the DSM prediction with experimental data for elongation rates  $\dot{\lambda}=5$ , 0.5, and 0.05 1/s.**

The symbols are experimental data and the solid lines are the DSM predictions. [Color figure can be viewed in the online issue, which is available at [wileyonlinelibrary.com](http://wileyonlinelibrary.com).]

relaxation time can be estimated to be  $\tau_d \approx 0.02$ s from the cross-over between  $G'$  and  $G''$  in Figure 3B. In the presence of network, this longest relaxation time goes up roughly by a factor of two due to the suppressed CD from the network chains, as can be observed in Figure 5A. The resulting Weissenberg number during the elongation experiment,  $Wi = \dot{\epsilon}\tau_d$ , is shown in the inset of Figure 6B. Note that according to this analysis, an elongation rate on the order of 100 1/s or greater would be required to observe a significant effect of the high-molecular-weight solvent in the nonlinear mechanical response of the swollen network blend. Even though the direct contribution of the dangling and solvent chains is very small, there is an indirect contribution via CD on the network chains. The black line in Figure 6A includes these effects.

The DSM predictions for the other two lower elongation rates,  $\dot{\lambda}=0.5$ , and 0.05 1/s are compared with experimental data<sup>3</sup> in Figure 7. For the lowest elongation rate, the agreement between experiments and predictions is very good. However, there is a significant discrepancy between the DSM prediction and the experimental data for the intermediate elongation rate. The data for this intermediate elongation rate (0.5 1/s) does not appear to be consistent with the other two rates. The stress for the intermediate rate is expected to lie between the stress for the lowest and the highest rate. Additionally, the behavior for this intermediate rate looks more Hookean (linear) than for the lowest rate which also indicates that the data-set for 0.5 1/s seems inconsistent. The inconsistencies in the data may have been caused by fracture of the test specimens (dog bones) during the elongation experiments, inhomogeneities, and so forth. Regardless of these inconsistencies at the intermediate rate, the good agreement for the highest and lowest rates allows us to conclude that the DSM can successfully predict the nonlinear elongation behavior of PDMS gels swollen with high molecular weight solvent.

## Conclusions

The composition of gels made of cross-linked PDMS swollen with high-molecular-weight PDMS solvent can be

tuned to produce materials with a large storage modulus and an enhanced loss modulus at high frequencies. More specifically, the mechanical properties of swollen network blends depend on the concentration of active network chains, the concentration of solvent, and the molecular weight distribution of each of the components. To characterize such a system, one needs a theory sufficiently robust that it can be applied to linear chains, star-branched chains, and cross-linked gels in both linear and nonlinear rheology. Although this is straightforward in the DSM, there is no such possibility in tube models.<sup>6,7</sup> Moreover, the parameters ( $\beta$ ,  $\tau_K$ ) can be determined from dynamic modulus data for the pure solvent. The fraction of active network strands was estimated by generalizing previous work by Khaliullin and coworkers<sup>20</sup> to account for polydispersity of the network chains. These parameters were then used to predict the linear and nonlinear rheology of the swollen network.

The DSM prediction for the dynamic modulus of the PDMS swollen gel was compared to experimental data reported by Mrozek et al.<sup>2</sup> We find that the DSM produces good quantitative predictions of the dynamic modulus of this complex system. Our results show that the effect of high-molecular-weight solvent becomes relevant in the overall dynamic modulus of the swollen network at frequencies above 1 Hz. In this frequency range, the amount of energy dissipation ( $G''$ ) is significantly increased due to the presence of the entangled solvent. We test the nonlinear rheological predictions of the DSM against elongation experiments of the swollen PDMS networks. We find that the DSM can predict well the experimental observations. Moreover, valuable insight into the specific dynamics of each component in this complex blend is gained. This allows us to conclude that even at the highest elongation rates at which experiments have been performed, the contribution of the high molecular weight solvent to the overall mechanical response of the blend is negligible. More experimental results are required to validate this conclusion.

The good quantitative agreement of the DSM predictions with experimental results indicates that the model can be used as a computational tool<sup>28</sup> to design swollen gel formulations with tailored mechanical properties for specific applications. The same type of modeling presented in this work can be easily further developed to include other polymer architectures such as star-branched solvents, which will broaden the spectrum of mechanical properties that can be achieved with these types of swollen polymeric gels.

## Acknowledgments

The authors are grateful to the Army Research Office (W911NF-08-2-0058 and W911NF-09-2-0071) for financial support. M. Katzarova thanks Andrés Córdoba for insightful discussions.

## Literature Cited

- Kalcioglu ZI, Mrozek RA, Mahmoodian R, VanLandingham MR, Lenhart JL, Van Vliet KJ. Tunable mechanical behavior of synthetic organogels as biofidelic tissue simulants. *J Biomech.* 2013;46:1583–1591.
- Mrozek RA, Cole PJ, Otim KJ, Shull KR, Lenhart JL. Influence of solvent size on the mechanical properties and rheology of polydimethylsiloxane-based polymeric gels. *Polymer.* 2011;52:3422–3430.
- Slizberg YR, Mrozek RA, Schieber JD, Kröger M, Lenhart JL, Andzelm JW. Effect of polymer solvent on the mechanical



- properties of entangled polymer gels: coarse-grained molecular simulation. *Polymer*. 2013;54:2555–2564.
4. Sirk TW, Slizoberg YR, Brennan JK, Lisal M, Andzelm JW. An enhanced entangled polymer model for dissipative particle dynamics. *J Chem Phys*. 2012;136:134903.
  5. Slizoberg YR, Andzelm JW. Fast protocol for equilibration of entangled and branched polymer chains. *Chem Phys Lett*. 2012;523:139–143.
  6. Masubuchi Y, Ianniruberto G, Greco F, Marrucci G. Entanglement molecular weight and frequency response of sliplink networks. *J Chem Phys*. 2003;119:6925–6930.
  7. Rubinstein M, Panyukov S. Elasticity of polymer networks. *Macromolecules*. 2002;35:6670–6686.
  8. Lin DC, Douglas JF, Horkay F. Development of minimal models of the elastic properties of flexible and stiff polymer networks with permanent and thermoreversible cross-links. *Soft Matter*. 2010;6:3548–3561.
  9. Carrillo J-MY, MacKintosh FC, Dobrynin AV. Nonlinear elasticity: from single chain to networks and gels. *Macromolecules*. 2013;46:3679–3692.
  10. Sakai T, Kurakazu M, Akagi Y, Shibayama M, Chung U-I. Effect of swelling and deswelling on the elasticity of polymer networks in the dilute to semi-dilute region. *Soft Matter*. 2012;8:2730–2736.
  11. Saalwächter K, Chassé W, Sommer J-U. Structure and swelling of polymer networks: insights from NMR. *Soft Matter*. 2013;9:6587–6593.
  12. Kawamura T, Urayama K, Kohjiya S. Multiaxial deformations of end-linked poly (dimethylsiloxane) networks. III. Effect of entanglement density on strain-energy density function. *J Polym Sci Part B: Polym Phys*. 2002;40:2780–2790.
  13. Schieber J. Fluctuations in entanglements of polymer liquids. *J Chem Phys*. 2003;118:5162–5166.
  14. Schieber JD, Neergaard J, Gupta S. A full-chain, temporary network model with sliplinks, chain-length fluctuations, chain connectivity and chain stretching. *J Rheol*. 2003;47:213.
  15. Khaliullin RN, Schieber JD. Analytic expressions for the statistics of the primitive-path length in entangled polymers. *Phys Rev Lett*. 2008;100:188302.
  16. Khaliullin RN, Schieber JD. Self-consistent modeling of constraint release in a single-chain mean-field slip-link model. *Macromolecules*. 2009;42:7504–7517.
  17. Khaliullin RN, Schieber JD. Application of the slip-link model to bidisperse systems. *Macromolecules*. 2010;43:6202–6212.
  18. Pilyugina E, Andreev M, Schieber JD. Dielectric relaxation as an independent examination of relaxation mechanisms in entangled polymers using the discrete slip-link model. *Macromolecules*. 2012;45:5728–5743.
  19. Andreev M, Khaliullin RN, Steenbakkers RJ, Schieber JD. Approximations of the discrete slip-link model and their effect on nonlinear rheology predictions. *J Rheol*. 2013;57:535.
  20. Jensen MK, Khaliullin R, Schieber JD. Self-consistent modeling of entangled network strands and linear dangling structures in a single-strand mean-field slip-link model. *Rheol Acta*. 2012;51:21–35.
  21. Morrison FA. *Understanding Rheology*. Oxford University Press, New York, 2001.
  22. Bird RB, Armstrong RC, Hassager O. *Dynamics of Polymeric Liquids. Vol. 1: Fluid Mechanics*. New York, NY: Wiley, 1987.
  23. Schieber JD. Generic compliance of a temporary network model with sliplinks, chain-length fluctuations, segment-connectivity and constraint release. *J Non-Equilib Thermodyn*. 2003;28:179–188.
  24. Guzmán JD, Schieber JD, Pollard R. A regularization-free method for the calculation of molecular weight distributions from dynamic moduli data. *Rheol Acta*. 2005;44:342–351.
  25. Rubinstein M, Colby RH. *Polymer Physics*. Oxford University Press, New York, 2003.
  26. Baumgaertel M, Schausberger A, Winter H. The relaxation of polymers with linear flexible chains of uniform length. *Rheol Acta*. 1990;29:400–408.
  27. Andreev M, Hualong F, Yang L, Schieber JD. Universality and speed-up in equilibrium and non-linear rheology predictions of the Fixed Slip-Link Model. In press.
  28. Salib IG, Kolmakov GV, Bucior BJ, Peleg O, Kröger M, Savin T, Vogel V, Matyjaszewski K, Balazs AC. Using mesoscopic models to design strong and tough biomimetic polymer networks. *Langmuir*. 2011;27:13796–13805.

Manuscript received Oct. 9, 2013, and final revision received Jan. 11, 2014.